scientific reports

Check for updates

OPEN

Malabaricone C isolated from edible plants as a potential inhibitor of SARS-CoV-2 infection

Mutmainah[1], Yuta Murai[1,2,3]✉, Ai Fujimoto[1], Rintaro Kawamura[1], Akira Kitamura[1,2], Sajeer Koolath[1], Seigo Usuki[2], Michihito Sasaki[4,5], Yasuko Orba[4,5,6], Yasuyuki Igarashi[2], Hirofumi Sawa[4,5,6], Akihiko Sato[4,5,7]✉ & Kenji Monde[1,2]✉

Although the SARS-CoV-2 epidemic worldwide has gradually decreased, in some areas, the situation has not yet been stamped and has become a global health emergency. It is quite possible that we could again be threatened by a new coronavirus. Therefore, new nucleotide analog drugs and vaccines or using drug repositioning for SARS-CoV-2 still has been developed, yet their safety and efficacy against COVID-19 remains underexplored. Malabaricone C is 2,6-dihydroxyphenyl acylphenol found in edible plants such as the mace spice of nutmeg derived from the seeds of *Myristica fragrans*. In this study, we identified malabaricone C as the first inhibitor of SARS-CoV-2 from natural food with a safe alternative for drugs. Malabaricone C and its chemical derivatives showed EC_{50} values of 1–1.5 µM against SARS-CoV-2 (WK-521, ancestral strain) and its variant strains in mammalian cells (HEK293T and Vero E6). In addition, we have successfully established novel evaluation system for the inhibition of SARS virus cell fusion by visualization for providing a versatile tool for study SARS-CoV-2 mediated fusion. Furthermore, our experiments suggested that malabaricone C could affect the distribution of sphingomyelin on the plasma membrane, which involves in viral infections. Thus, in light of the beneficial effect of malabaricone C on viral infection, the nontoxic malabaricone C is a suitable candidate as a drug that can be employed in the treatment and prevention of COVID-19. Moreover, it may potentially be used to treat acute infections of other enveloped viruses.

Coronaviruses are enveloped, positive-sense, single-stranded RNA viruses that infect a wide range of hosts including reptiles, birds, and mammals. Severe Acute Respiratory Syndrome-Coronavirus-2 (SARS-CoV-2), the third most highly pathogenic coronavirus identified after SARS-CoV and Middle East respiratory syndrome coronavirus (MERS-CoV) in the twenty-first century, emerged in Wuhan, China in late 2019. It has rapidly spread and has become a global health emergency[1]. Coronavirus disease 2019 (COVID-19), caused by SARS-CoV-2 shows respiratory disturbance symptoms such as cough, fever, and serious pneumonia leading to death[2,3]. Although the incidence of COVID-19 has gradually decreased worldwide, some countries and regions are still experiencing outbreaks of new variants and spread of infection. During the SARS-CoV-2 pandemic, the molecular mechanisms of infection of SARS-CoV-2 in host cells were gradually elucidated. In the initial step, the surface unit S1 of the virus spike (S) glycoprotein is cleaved and binds to angiotensin-converting enzyme 2 (ACE2). In the second step, to provide unit S2 for fusion to host cell membranes, S1/S2 and S2' sites of S glycoproteins need to be proteolytically cleaved by the host cell protease transmembrane serine protease 2 (TMPRSS2-pathway) (Fig. 1)[4]. In addition, other candidates, such as neuropilin 1 as a co-receptor, and cathepsin L, TMPRSS11D, and TMPRSS13, have been proposed to be related to SARS-CoV-2 infection as well[5678]. However, the details regarding the pathogenesis of SARS-CoV-2 remain unclear. Therefore, the accurate inhibition of SARS-CoV-2 infection remains a challenge. The development of new mRNA vaccines has brought about significant benefits against anti-SARS-CoV-2, whereas the RNA vaccines are associated with side effects,

[1]Graduate School of Life Science, Hokkaido University, Kita 21 Nishi 11, Kita-Ku, Sapporo 001-0021, Japan. [2]Faculty of Advanced Life Science, Hokkaido University, Kita 21 Nishi 11, Kita-Ku, Sapporo 001-0021, Japan. [3]Division of Applied Bioscience, Graduate School of Agriculture, Hokkaido University, Kita 9, Nishi 9, Kita-Ku, Sapporo, Hokkaido 060-8589, Japan. [4]International Institute for Zoonosis Control, Hokkaido University, Kita 20 Nishi 10, Kita-Ku, Sapporo 001-0020, Japan. [5]Institute for Vaccine Research and Development, Hokkaido University, Kita 21 Nishi 11, Kita-Ku, Sapporo 001-0020, Japan. [6]One Health Research Center, Hokkaido University, Kita 20 Nishi 10, Kita-Ku, Sapporo 001-0020, Japan. [7]Laboratory for Drug Discovery & Disease Research, Shionogi & Co., Ltd., 3-1-1, Futaba-tyo, Toyonaka, 561-0825, Japan. ✉email: ymurai@agr.hokudai.ac.jp; akihiko.sato@shionogi.co.jp; kmonde@sci.hokudai.ac.jp

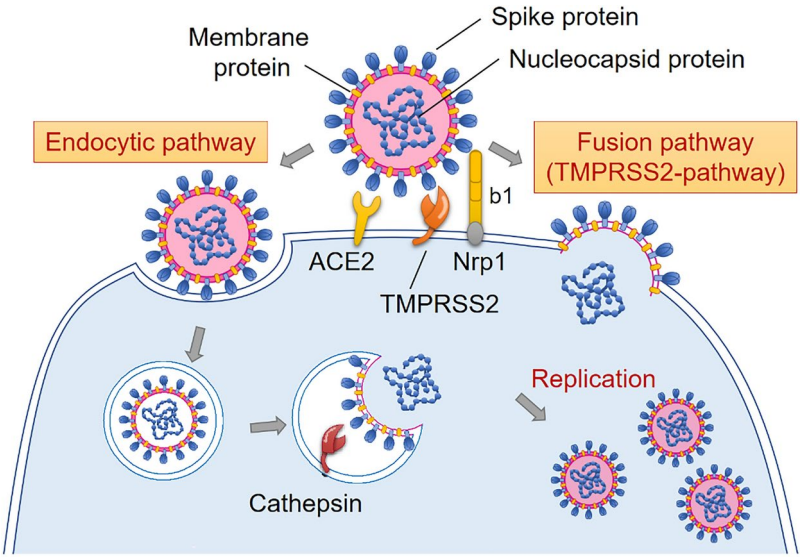

Fig. 1. Fusion of SARS-CoV-2 occurs through endocytic and fusion (TMPRSS2) pathways.

such as headache, skin discoloration, weakness/fatigue, and hypersensitivity allergic reaction[9]. Besides, antiviral drugs against SARS-CoV-2 are still in their immature phase. However, several approved repositioned materials and investigational drugs have been used for their antiviral activities against SARS-CoV-2. For example, remdesivir (GS5734), a monophosphoramidate prodrug with an adenosine analog for Ebola[10]and Marburg viruses, has been recognized as an antiviral drug against enveloped viruses (SARS/MERS-CoV)[11] in vivo. Xiao et al. reported that remdesivir exhibits potent antiviral activity against SARS-CoV-2 at a low micromolar concentration (EC_{50} = 0.77 μM) in Vero E6 cells[12]. Before long, the use of remdesivir in COVID-19 had received emergency use authorization from the FDA. However, owing to limited alternatives and high-risk side effects, the development of improved therapeutic agents is urgently required. Therefore, it takes many years to obtain evidence of the efficacy and side effects of these antiviral drugs and vaccines. With the exception of Food and Drug Administration-approved drugs, natural products with medical applications have gained considerable attention. Therefore, from a safety perspective, the bioactive compounds found in food and edible gradients are attractive and promising candidates for the discovery of new drugs against SARS-CoV-2. Several naturally occurring compounds are currently being investigated for their applications in the inhibition of SARS-CoV-2 infection, and many research groups have discovered the therapeutic potential of these compounds. Rao et al. reported that the phytochemical shikonin could be a promising drug target against the main protease of SARS-CoV-2, which regulates viral replication and transcription[13]. In another study, flavonoids, including myricitrin and licoleafol, were introduced as inhibitors of the chymotrypsin-like protease of SARS-CoV-2 based on the predicted 3D structure[14]. Panduratin A extracted from *Boesenbergia rotunda*, a promising anti-SARS-CoV-2 agent, was also reported by using a high-content imaging system coupled with a plaque reduction assay, has also been reported by Borwornpinyo and Thitithanyanont[15]. In addition, there have been reports on the search for inhibitors from natural products to create more effective inhibitors for new coronavirus variants that must emerge in the future[16171819]. However, although these results are encouraging, there is insufficient safety data to confirm the benefits and potential of these materials. In addition, naturally occurring compounds in foods are recognized as SARS-CoV-2 drug targets[20]. Recently, gingkolic acid, a natural compound isolated from *Ginkgo biloba*, has been shown to inhibit the cell fusion of enveloped viruses and viral DNA and protein synthesis[21]. We have also demonstrated that ginkgolic acid has highly potent inhibitory activity toward sphingomyelin synthase (SMS), modulating sphingomyelin levels in lipid membrane fluidity and signal transduction[222324], by our group[25]. In addition, SMS is related to the generation and release of influenza virus particles in the human haploid cell line[26]and is involved in HIV-1 Env-mediated membrane fusion[27]. Therefore, modulation of SMS activity could be a novel therapeutic approach for enveloped viral infections. To date, we have reported naturally occurring SMS modulatory compounds, daurichromenic acid from the Chinese traditional medicinal plant *Rhododendron dauricum*[28], and malabaricone C from the fruits of *Myristica cinnamomea*[29]. The latter inhibitors may be especially safe, with fewer side effects than other SMS inhibitors because they were isolated from an edible fruit. In addition, we have already proven the multiple efficacies in reducing weight gain, improving glucose tolerance, and reducing hepatic steatosis in high fat diet-induced obesity mice models by oral intake of malabaricone C[29]. In the present study, we demonstrated the ability of malabaricone C and its organic synthesis derivatives to inhibit SARS-CoV-2 infection and fusion with Vero E6/TMPRSS2 cells, as determined by MTT and fusion assays. Our new findings demonstrate the potential ability of malabaricones to inhibit SARS-CoV-2 infection, which could attract much interest in the development of prospective drugs towards SARS-CoV-2.

Results

Malabaricone C and its derivatives with potential anti-SARS-CoV-2

To measure the inhibitory activities of ginkgolic acid, malabaricone C, and daurichromenic acid towards SARS-CoV-2 (WK-521, ancestral strain), we conducted an MTT assay using Vero E6 cells that stably express TMPRSS2 (Vero E6/TMPRSS2) are highly susceptible to SARS-CoV-2 infection[30] (Figure S1). Ginkgolic acid showed moderate inhibition of SARS-CoV-2 infection in Vero E6/TMPRSS2 cells, with an EC_{50} of 7.9 µM. Malabaricone C showed potential inhibitory activity against SARS-CoV-2 (WK-521) replication into VeroE6/TMPRSS2 cells (EC_{50} = 1.5 µM, Figure S2). Next, to investigate the possibility of a highly potent inhibitory activity against SARS-CoV-2, structure–activity relationship (SAR) studies of the malabaricone C scaffold were performed. The reduction of the carbonyl group (2) and various modifications, such as esterification (acetyl (3, 4) and benzoyl (5, 6)) and etherification (methyl and benzyl) of the hydroxy groups on the aromatics, were achieved (Fig. 2). Furthermore, the SAR of the chain length between the two aromatic rings could be another point of interest for

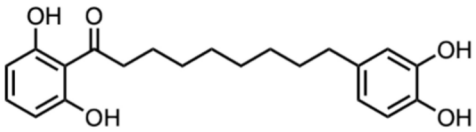

malabaricone C, **1**

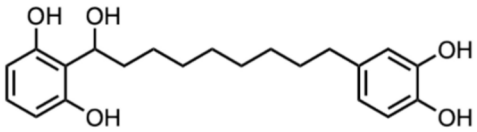

2

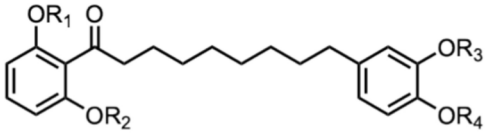

3 - 10

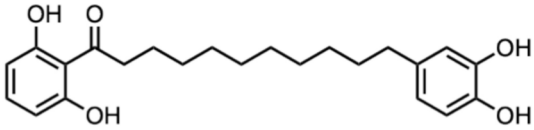

11

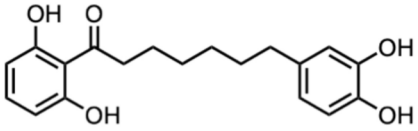

12

Compound	R_1	R_2	R_3	R_4
3	Ac	Ac	Ac	Ac
4	Ac	Ac	Ac (H)	H (Ac)
5	Bz	Bz	Bz	Bz
6	Bz	Bz	Bz (H)	H (Bz)
7	Me	Me	Me	Me
8	Me	Me	Me (H)	H (Me)
9	H	Bn	Bn	Bn
10	Bn	Bn	Bn (H)	H (Bn)

Fig. 2. Derivatization of malabaricone C for SAR study.

the altered activity. Malabaricone C with shorter or longer alkyl chains of malabaricone C were synthesized as reported by Tsuda et al.[31] with slight modifications (Scheme S1).

The antiviral activity of the derivatized malabaricone C compounds was evaluated using the same MTT assay. The reduced carbonyl group compound 2 exhibited slightly decreased activity compared with malabaricone C. Esterification and etherification of the hydroxy group compounds (3, 4, 6, and 8) retained SARS-CoV-2 inhibitory activity. Interestingly, the modification of both hydroxyl groups on the catechol ring (5 and 7) reduced their inhibitory activities, suggesting that the hydroxyl groups of the catechol ring have a significant effect on its activity. In contrast, the tetrabenzylated compound (9) showed a dramatic loss of activity. Partial benzyl modification (10) also reduced the antiviral activity (Table 1., Figure S3). However, this mechanism remains unclear, suggesting the need for further detailed investigation. Additionally, the chain length between the two aromatic rings significantly affected the activity; the two-carbon longer chain 11 dramatically showed less potent antiviral activity than the two-carbon shorter chain 12. Therefore, the carbonyl group and the appropriate chain length between the two aromatic rings are essential for the inhibition of SARS-CoV-2 replication. Moreover, the esterification and etherification of malabaricone C had little effect on its inhibitory activity.

Anti-SARS-CoV-2 variants effect of malabaricone C in human embryonic kidney cells 293

To explore the inhibition of SARS-CoV-2 replication by malabaricone C and its derivatives during human infection, we examined their antiviral activity against the SARS-CoV-2 alpha (B.1.1.7), SARS-CoV-2gamma (P.1), and SARS-CoV-2 delta (B.1.617.2) variants using human embryonic kidney cells 293 (HEK293TA) through the MTT assay. As with WK-521, malabaricone C and some of its derivatives also exhibited potent anti-SARS-CoV-2 activity with an IC_{50} of 1.5 – 2.0 μM(Table 2).

Novel visualization of fusion assay for SARS-CoV-2 Furthermore, to establish a visual evaluation system for the inhibitory effect of inhibitors against SARS-CoV-2 entry into uninfected cells, we established a novel cell-to-cell fusion assay. For this purpose, a persistent SARS-CoV-2 infected cell line and a HEK293TA cell line expressing green fluorescent protein (GFP) or mCherry protein were prepared. Figure 3A illustrates the underlying concept wherein yellow hypertrophy cells appear when cell-to-cell fusion occurs, whereas green and red colored HEK293TA cells are observed when inhibition by antiviral agents occurs. Thus, the inhibitory effect can be evaluated using the number and total area of cells emitting yellow fluorescence as indices, compared to the virus control in the presence of SARS-CoV-2 without inhibitors (VC).

Next, to investigate the inhibitory effect of malabaricones on the fusion assay, cells were treated with malabaricone C and its derivatives (3 and 6) at concentrations ranging from 0.8 to 25 μM. The inhibition of cell fusion increased in a dose-dependent manner, as determined by calculating the intensity of yellow hypertrophic cells (Fig. 3B, C). The EC_{50} values of all inhibitors were similar to those in the MTT assay. In addition, these compounds prevented the SARS-CoV-2δ variant as well (Supplementary Data Movie). Therefore, this cell–cell fusion assay is a simple and versatile tool for study SARS-CoV-2 mediated fusion.

Visualization of the distribution of sphingomyelin on the plasma membrane The regulation of SMS activity is crucially related to the cell membrane fusion of envelope viruses[2627]. Lipid rafts, enriched in sphingomyelin (SM) clusters on the plasma membrane, have crucial essential biological functions related to membrane signaling and protein trafficking[3233]. In addition, recent studies have reported that lipid rafts are an important location for enveloped viral infection[34]. Thus, the distribution of SM in the plasma membrane and its involvement in viral

Compound	SARS-CoV-2 (WK-521, ancestral strain)		
	EC_{50} (μM)	CC_{50} (μM)	Selectivity index
1	1.5	14	9.7
2	5.4	>40	>7.4
3	1.3	16	12
4	1.5	15	10
5	14	>40	>2.8
6	1.0	6.8	6.8
7	6.0	27	4.6
8	1.5	5.5	3.7
9	n.d.	n.d.	-
10	21	>40	>1.8
11	14	32	2.3
12	2.9	41	14.2
Remdesivir	0.5	>10	>19.9
Molnupiravir	0.15	5.3	33.8

Table 1.. Structure–activity relationship of malabaricone C derivatives in the inhibition of SARS-CoV-2 (WK-521) infection. The concentration numbers indicate the EC_{50}, CC_{50} and selectivity index values, respectively. These values were calculated using an MTT assay system. Results are presented as means, and experiments were repeated at least 3 times. (n.d. = not determined)

Compound	SARS-CoV-2α		
	EC_{50} (μM)	CC_{50} (μM)	Selectivity index
1	1.9	5.2	2.6
2	7.3	12	1.7
3	1.4	6.2	4.3
4	1.4	6.1	4.1
6	1.5	3.2	2.1
11	5.2	24	4.7
12	2.9	6.5	2.2
Remdesivir	< 0.078	0.5	> 6.7
Molnupiravir	0.4	6.1	14.7
Compound	**SARS-CoV-2γ**		
	EC_{50} (μM)	CC_{50} (μM)	Selectivity index
1	1.7	6.2	3.6
2	6.8	16	2.4
3	1.5	6.4	4.3
4	1.3	6.6	4.8
6	1.6	2.9	1.7
11	16	22	1.4
12	7.2	10	1.5
Remdesivir	< 0.078	0.7	> 9.3
Molnupiravir	0.52	6.7	13
Compound	**SARS-CoV-2δ**		
	EC_{50} (μM)	CC_{50} (μM)	Selectivity Index
1	1.9	6.5	3.4
2	8.3	23	2.7
3	1.4	6.4	4.5
4	1.6	6.7	4.1
6	0.71	2.9	4
11	7.3	19	2.6
12	4.3	10	2.3
Remdesivir	< 0.078	0.7	> 9.3
Molnupiravir	0.45	5.9	13

Table 2. Malabaricone C and its derivatives in the inhibition of infection by SARS-CoV-2 variants. The concentration numbers indicate the EC_{50}, CC_{50} and selectivity index values, respectively. These values were calculated using an MTT assay system. Results are presented as means and experiments were repeated at least 2–3 times.

infections have attracted academic interest. To understand the biological mechanism underlying the inhibition of SARS-CoV-2 infection by malabaricone C, we examined the distribution of SM on the plasma membrane in Vero E6 cells with EGFP-conjugated specific SM-binding proteins, lysenin (Lys) and equinatoxin II (EqtII) that can recognize different membrane distributions of SM Lys binds clustered SM, whereas EqtII preferentially binds dispersed SM[35,36]. As shown in Fig. 4, the fluorescence intensity of EGFP-NT-Lys on the plasma membrane after treatment with malabaricone C was lower than that of the control. However, there was almost no difference in the fluorescence intensity of EqtII-EGFP between malabaricone C treatment and the control. It was inferred that malabaricone C affected the composition of lipid rafts in the plasma membrane. Therefore, the inhibition of SARS-CoV-2 entry by malabaricone C was suggested to occur by interfering with the assembly of lipid rafts on the cell membrane.

Discussion

In summary, malabaricone C and its derivatives were identified as natural inhibitors of anti-SARS-CoV-2 (WK-521) agents, similar to remdesivir, in Vero E6/TMPRSS2 cells. In particular, malabaricone C and compounds (3), (4), and (6) had a large selective index of over five values between EC_{50} and CC_{50}. Interestingly, those compounds exhibited potent antiviral effect against SARS-CoV-2 variants with an EC_{50} of 1.5–2.0 μM, and their antiviral activities were equal to or even more potent than those of chloroquine and hydroxychloroquine, the anti-SARS-CoV-2 drugs that have been FDA-approved for COVID-19 treatment[37,38,39]. We also investigated the anti-SARS-CoV-2 variants (B.1.1.7, P.1, and B.1.617.2) activity of malabaricone C and its derivatives in human embryonic kidney cells HEK293TA cell lines. These results emphasize the potential implications of malabaricone C and its derivatives as novel anti-SARS-CoV-2 candidates for the treatment of COVID-19. In

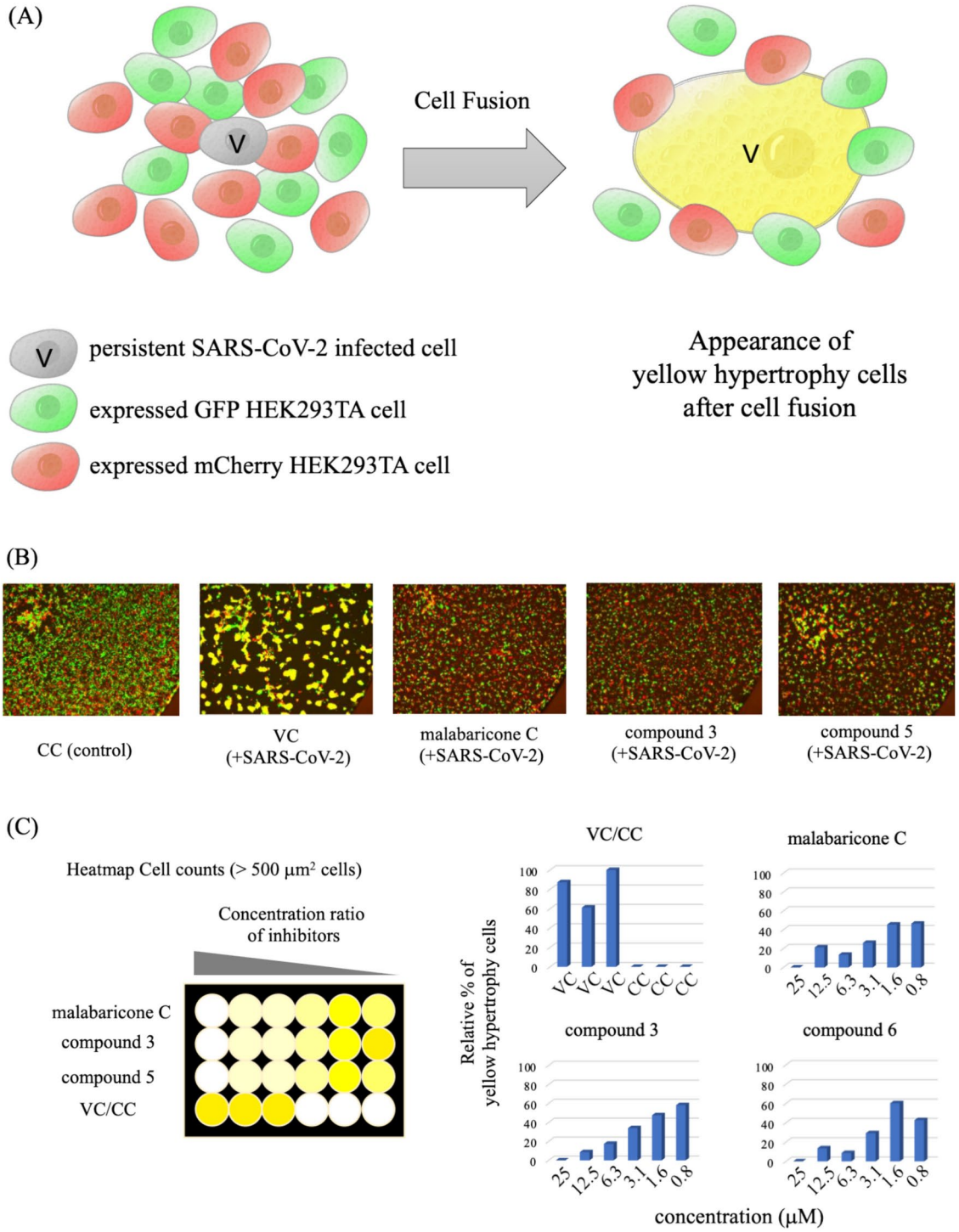

Fig. 3. Illustration of the fusion assay for SARS-CoV-2. Cell control (CC) was conducted with only assay medium. Virus control (VC) was conducted in the presence of SARS-CoV-2 without inhibitors. (**A**) Concept of the visualized fusion assay for SARS-CoV-2. The persistent cells were turned yellow and hypertrophied by cell fusion with two types of cells that introduced GFP and mCherry. (**B**) Scanning micrographs (×40) of the fusion assay in the presence of each inhibitor at 12.5 μM after 24 h. (**C**) The fusion inhibition of Malabaricone C and its derivatives was measured by counting the number of yellow hypertrophy cells (> 500 μm^2) (n = 2 biological replicates).

addition, we established a novel visualized cell fusion assay for SARS-CoV-2 with SARS-CoV-2 persistently infected HEK293TA-G cells (green fluorescence) and HEK293TA-M cells (red fluorescence). This simple cell–cell fusion assay provides a versatile tool for study SARS-CoV-2 mediated fusion. Currently, there are no reports on the molecular mechanisms of infection between SARS-CoV-2 and host cells[40]. However, the molecular and

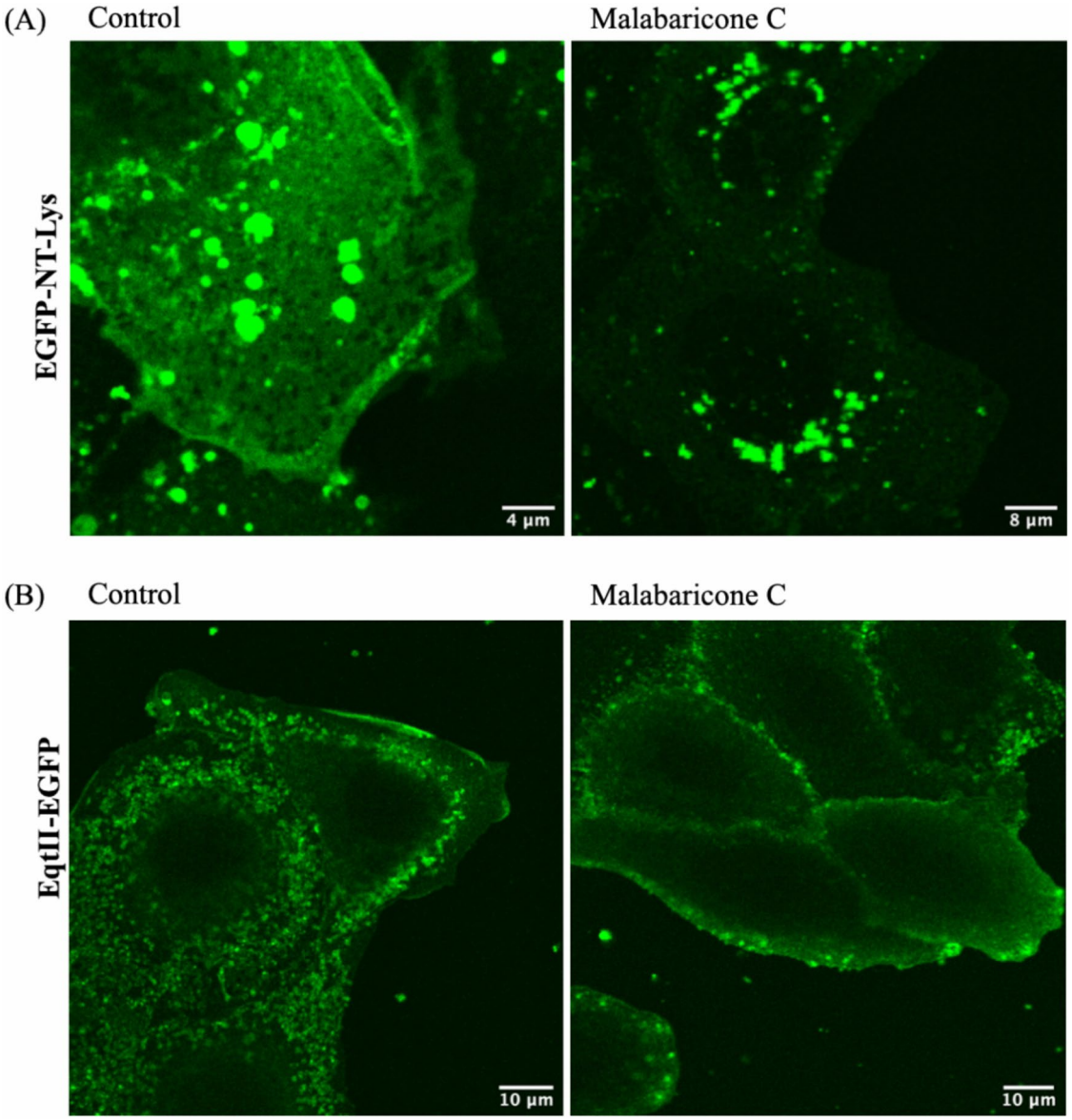

Fig. 4. Sphingomyelin (SM) cluster on the plasma membrane stained by EGFP conjugated lysenin (EGFP-NT-Lys) and equinatoxin II (EqtII-EGFP). Vero E6 cells were treated with malabaricone C or DMSO (control). (**A**–**B**) Cells were fixed and incubated with EGFP-NT-Lys (**A**) or EqtII-EGFP (**B**) at 4 °C overnight and examined by confocal microscopy.

cellular mechanisms of malabaricone C antiviral activity have not been completely elucidated. Here, we first demonstrated the partial mechanism of the anti-SARS-CoV-2 activity of malabaricone via interference with lipid raft formation on the plasma membrane in Vero E6 cells. Further detailed elucidation of the mechanism is required. Finally, while existing SARS-CoV-2 antiviral drugs are often associated with side effects (liver dysfunction, hypotension and teratogenicity so on),

malabaricone C is present in various edible plants, which can be safely and easily administered to the elderly and small children for prevention of COVID-19 as an alternative to antiviral drugs or vaccines. Although this study exhibited the effects of malabaricone C towards the distribution of sphingomyelin in the plasma membrane, there are still issues to be investigated in more detail to evaluate the viral infection by the physiological phenomenon. To assess the issues, this finding could be a valuable approach for new drug development based on the malabaricone C structure and applied to assessment of studies in animal models of COVID-19 in the future.

Methods

Generation of TMPRSS2- and ACE2- expressing cells

Vero E6 cells (CRL-1586, ATCC, VA 20,110. USA) stably expressing human TMPRSS2 (Vero E6/TMPRSS2) and HEK293TA cells (RCB2202: RIKEN BRC, Tokyo, Japan) stably expressing human ACE2 have been described previously (Sasaki et al. *PLoS Pathogens*2021)[30], (Uemura et al. *Scientific Reports*2021)[41]. MA104T cells stably

expressing human TMPRSS2 were established from the African green monkey kidney-derived cell line MA104 (RCB0994; RIKEN BRC, Tokyo, Japan) by lentiviral vector transduction with CSII-CMV-TMPRSS2-IRES2-Bsd. To prepare the lentiviral particles, the lentiviral vector plasmid and lentiviral high-titer packaging mix (Takara Bio, Shiga, Japan) were transfected into Lenti-X 293 T cells using TransIt-293 transfection reagent (Mirus Bio, Madison, WI).

Generation of HEK293TA-G and HEK293TA-M cells

HEK293TA cells stably expressing AcGFP1 and mCherry were established by lentiviral vector transduction as follows. AcGFP1 and mCherry coding sequences were subcloned into pLVSIN-CMV Pur and pLVSIN-CMV Neo (Takara Bio), respectively. The resultant plasmids were used for lentiviral vector preparation as described above.

Generation of persistent SARS-CoV-2 infection cells

MA104T cells were infected with SARS-CoV-2 (WK-521) and cultured in an exchange medium on a regular basis. After apparent cytopathic effect (CPE), the surviving cells were maintained with regular medium exchange for approximately 4 weeks. MA104T cells persistently infected with SARS-CoV-2 continuously proliferate and release infectious SARS-CoV-2.

Virus preparation

SARS-CoV-2 strain WK-521 (Ancestral, Pango Lineage: A, GISAID: EPI_ISL_408667), QK002 (Alpha, Pango Lineage: B.1.1.7, GISAID: EPI_ISL_768526), TY7-501 (Gamma, Pango Lineage: P.1, GISAID: EPI_ISL_833366), TY11-927 (Delta, Pango Lineage: B.1.617.2, GISAID: EPI_ISL_2158617), were provided by the National Institute of Infectious Diseases, Tokyo, Japan. The virus stock was propagated in Vero E6/TMPRSS2 cells and titrated by inoculating Vero E6/TMPRSS2 cells in a 96-well plate with five-fold serial dilutions of the virus, and CPE was scored to calculate the TCID50/ml.

SARS-CoV-2 inhibition MTT assay

An MTT (3-(4,5-di-methylthiazol-2-yl)−2,5-diphenyltetrazolium bromide, yellow tetrazole) (5 mg/mL; Nacalai Tesque) assay was performed to evaluate cell viability following viral infection. Vero E6/TMPRSS2 or HEK293TA cells ($2.0 – 2.5 \times 10^4$ cells/mL) were plated on 96-well microplates in MEM containing 2% FBS and the test compounds. Either WT or variants of SARS-CoV-2 (50 µL/well) were added to the plates and then the cells were cultured for 2– 3 days. Subsequently, the MTT test solution was added to each well, and the cells were incubated for 4–6 h. After removing the solution and adding the cytolysis solution to each well, the plate was incubated at room temperature overnight. Absorbance was measured at 570 and reference wavelength of 630 nm using a Multiskan microplate reader (Thermo Fisher Scientific), and the 50% effective concentration (EC_{50}) was calculated. Cell toxicity was assessed using the same method as that used for the viral inhibitory assay, and the 50% cytotoxicity concentration (CC_{50}) was calculated.

SARS-CoV-2 fusion inhibition assay

SARS-CoV-2 persistently infected cells were seeded at 100 µL (1×10^4 cells)/well into a 96-well plate containing the inhibitors, then reacted at room temperature for 1 h. Subsequently, HEK293TA-G cells at 50 µL (5×10^4 cells)/well and HEK293TA-M cells at 50 µL (5×10^4 cells) /well were added to each well, mixed with a plate mixer, and then cultured in a CO_2 incubator for 24 h. By cell fusion of SARS-CoV-2 persistently infected cells, HEK293TA-G cells (green fluorescence), and HEK293TA-M cells (red fluorescence), hypertrophy cells were formed and emit yellow fluorescence. The cell fusion inhibitory effect was evaluated using the number and total area of cells emitting yellow fluorescence as indices. Fluorescent cells were counted using an all-in-one fluorescence microscope BZ-X800 (manufactured by KEYENCE).

Visualization of the distribution of sphingomyelin

EGFP-NH-Lys and EqtII-EGFP were prepared according to methods described by Bhat et al[31].. Vero E6 cells were seeded at 1.0×10^4 cells in a microplate suitable for confocal microscopy and cultured at 37 °C for 24 h. The cells were washed with PBS and treated with 5 µM malabaricone C in DMEM supplemented with 10% FBS and 1% penicillin/streptomycin at 37 °C for 30 min. The medium was removed, and the cells were fixed in 4% paraformaldehyde in PBS at 37 °C for 2 min and continued at room temperature for 30 min in a light-shielded condition. The cells were washed thrice with TBS, treated with blocking buffer (3% BSA in PBS) at room temperature for 1 h, and washed thrice with PBS. Cells were then incubated with EGFP-NT-Lys (25 µg/ml) or EqtII-EGFP (25 µg/ml) at 4 °C overnight and washed with PBS three times. After washing, the cells were observed under a confocal microscope.

Data availability

All data generated or analyzed during this study are included in this published article (and its Supplementary Information Files).

Received: 23 October 2024; Accepted: 16 December 2024
Published online: 12 March 2025

References

1. Zhu, N.; Zhang, D.; Wang, W.; Li, X.; Yang, B.; Song, J.; Zhao, X.; Huang, B.; Shi, W; Lu, R.; et al. A Novel Coronavirus from Patients with Pneumonia in China, 2019. *N. Engl. J. Med.* **382**, 727–733 (2020).
2. Li, Q.; Guan, X.; Wu, P.; Wang, X.; Zhou, L.; Tong, Y.; Ren, R.; Leung, K. S. M.; Lau, E. H. Y.; Wong, J. Y. et al., Early Transmission Dynamics in Wuhan, China, of Novel Coronavirus-Infected Pneumonia. *N. Engl. J. Med.* **382**, 1199–1207 (2020).
3. Sohrabi, C. et al. *Int. J. Surg.* **76**, 71–76 (2020).
4. Shang, J. et al. Cell entry mechanisms of SARS-CoV-2. *Proc. Natl. Acad. Sci. USA* **117**, 11727–11734 (2020).
5. Cantuti-Castelvetri, L. et al. Neuropilin-1 facilitates SARS-CoV-2 cell entry and infectivity. *Science.* **370**, 856–860 (2020).
6. Daly, J. L. et al. *Science.* **370**, 861–865 (2020).
7. Hoffmann, M. et al. Camostat mesylate inhibits SARS-CoV-2 activation by TMPRSS2-related proteases and its metabolite GBPA exerts antiviral activity. *EBioMedicine.* **65**, 103255 (2021).
8. Wei, J. et al. Genome-wide CRISPR Screens Reveal Host Factors Critical for SARS-CoV-2 Infection. *Cell.* **184**, 76–91 (2021).
9. Kadali, R. A. K. et al. Side effects of messenger RNA vaccines and prior history of COVID-19, a cross-sectional study. *Am J Infect Control.* **50**, 8–14 (2022).
10. Mulangu, S. et al. A Randomized, Controlled Trial of Ebola Virus Disease Therapeutics. *Engl. J. Med.* **381**, 2293–2303 (2019).
11. Sheahan, T. P.; Sims, A. C.; Graham, R. L.; Menachery, V. D.; Gralinski, L. E.; Leist, S. R.; Baric, R. S.; Case, J. B.; Pyrc, K.; Feng, J. Y. et al. Broad-spectrum antiviral GS-5734 inhibits both epidemic and zoonotic coronaviruses. *Sci. Transl. Med.* **9**, eaal3653 (2017).
12. Wang, M.; Zhang, L.; Yang, X.; Liu, J.; Xu, M.; Shi, Z.; Hu, Z.; Xiao, G.; Cao, R.; Zhong, Wu. Remdesivir and chloroquine effectively inhibit the recently emerged novel coronavirus (2019-nCoV) *in vitro*. **30**, 269–271 (2020).
13. Jin, Z. et al. Structure of M^{pro} from SARS-CoV-2 and discovery of its inhibitors. *Nature* **582**, 289–293 (2020).
14. Ul Qamar, M. T., Alqahtani, S. M., Alamri, M. A. & Chen, L. L. Structural basis of SARS-CoV-2 3CLproand anti-COVID-19 drug discovery from medicinal plants. *J. Pharm. Anal.* **10**, 313–319 (2020).
15. Kanjanasirirat, P. et al. High-content screening of Thai medicinal plants reveals Boesenbergia rotunda extract and its component Panduratin A as anti-SARS-CoV-2 agents. *Sci. rep.* **10**, 19963 (2020).
16. Rubio-Martínez, J. et al. Discovery of diverse natural products as inhibitors of SARS-CoV-2 Mpro protease through virtual screening. *J. Chem. Inf. Model.* **61**, 6094–6106 (2021).
17. Corona, A. et al. Natural compounds inhibit SARS-CoV-2 nsp13 unwinding and ATPase enzyme activities. *ACS Pharmacol. Transl. Sci.* **5**, 226–239 (2022).
18. Krüger, N. et al. Discovery of polyphenolic natural products as SARS-CoV-2 Mpro inhibitors for COVID-19. *Pharmaceuticals.* **16**, 190 (2023).
19. Risener, C. J. et al. Botanical inhibitors of SARS-CoV-2 viral entry: a phylogenetic perspective. *Sci. Rep.* **13**, 1244 (2023).
20. Romeo, I., Mesiti, F., Lupia, A. & Alcaro, S. Current Updates on Naturally Occurring Compounds Recognizing SARS-CoV-2 Druggable Targets. *Molecules.* **26**, 632 (2021).
21. Borenstein, R. et al. Ginkgolic acid inhibits fusion of enveloped viruses. *Sci. Rep.* **10**, 4746 (2020).
22. Bienias, K., Fiedorowicz, A., Sadowska, A., Prokopiuk, S. & Car, H. Regulation of Sphingomyelin Metabolism. *Pharmacol. Rep.* **68**, 570–581 (2016).
23. Mitsutake, S. et al. Dynamic Modification of Sphingomyelin in Lipid Microdomains Controls Development of Obesity, Fatty Liver, and Type 2 Diabetes. *J. Biol. Chem.* **286**, 28544–28555 (2011).
24. Yuyama, K., Sun, H., Mitsutake, S. & Igarashi, Y. Sphingolipid-Modulated Exosome Secretion Promotes Clearance of Amyloid-β by Microglia. *J. Biol. Chem.* **287**, 10977–10989 (2012).
25. Swamy, M. M. M. et al. Structure-inspired design of a sphingolipid mimic sphingosine-1-phosphate receptor agonist from a naturally occurring sphingomyelin synthase inhibitor. *Chem. Commun.* **54**, 12758–12761 (2018).
26. Tafesse, G. F. et al. Intact sphingomyelin biosynthetic pathway is essential for intracellular transport of influenza virus glycoproteins. *Proc. Natl. Acad. Sci. USA* **110**, 6406–6411 (2013).
27. Hayashi, Y. et al. Carboxyl-terminal tail-mediated homodimerizations of sphingomyelin synthases are responsible for efficient export from the endoplasmic reticulum. *J. Biol. Chem.* **292**, 1122–1141 (2017).
28. Deepak, V. H. et al. Daurichromenic acid from the Chinese traditional medicinal plant Rhododendron dauricum inhibits sphingomyelin synthase and Aβ aggregation. *Molecules* **25**, 4077 (2020).
29. Othman, M. A. et al. Malabaricone C as natural sphingomyelin synthase inhibitor against diet-induced obesity and its lipid metabolism in mice. *ACS Med. Chem. Lett.* **10**, 1154–1158 (2019).
30. Sasaki, M.; Uemura, K.; Sato, A.; Toba, S.; Sanaki, T. et al. SARS-CoV-2 variants with mutations at the S1/S2 cleavage site are generated in vitro during propagation in TMPRSS2-deficient cells. *PLoS Pathog.* e1009233 (2021).
31. Hosoi, S. et al. Synthesis and nematocidal activity of diarylnonanoids related to malabaricones. *Chem. Pharm. Bull.* **47**, 37–43 (1999).
32. Simons, K. & Ikonen, E. Functional rafts in cell membranes. *Nature.* **387**, 569–572 (1997).
33. Lingwood, D. & Simons, K. Lipid rafts as a membrane-organizing principle. *Science.* **327**, 46–50 (2010).
34. Suomalainen, M. Lipid rafts and assembly of enveloped viruses. *Traffic.* **3**, 705–709 (2002).
35. Bhat, H. B. et al. Binding of a pleurotolysin ortholog from Pleurotus eryngii to sphingomyelin and cholesterol-rich membrane domains. *J. Lipid Res.* **54**, 2933–2943 (2013).
36. Makino, A. et al. *FASEB J.* **29**, 477–493 (2015).
37. Gao, J., Tian, Z. & Yang, X. Breakthrough: chloroquine phosphate has shown apparent efficacy in treatment of COVID-19 associated pneumonia in clinical studies. *Biosci. Trends.* **14**, 72–73 (2020).
38. Yao, X. et al. In vitro antiviral activity and projection of optimized dosing design of hydroxychloroquine for the treatment of severe acute respiratory syndrome coronavirus 2 (SARS-CoV-2). *Clin. Infect. Dis.* **71**, 732–739 (2020).
39. Colson, P., Rolain, J. M., Lagier, J. C., Brouqui, P. & Raoult, D. Chloroquine and hydroxychloroquine as available weapons to fight COVID-19. *Int. J. Antimicrob. Agents.* **55**, 105932 (2020).
40. Zhang, Q. et al. Molecular mechanism of interaction between SARS-CoV-2 and host cells and interventional therapy. *Signal Transduct. Target. Ther.* **6**, 233 (2021).
41. Uemura, K. et al. MRC5 cells engineered to express ACE2 serve as a model system for the discovery of antivirals targeting SARS-CoV-2. *Sci. Rep.* **11**, 5376 (2021).

Acknowledgements

This work was partially supported by the Japan Agency for Medical Research and Development (AMED) under Grants JP243fa627005, a Grant-in-Aid for Scientific Research KAKENHI (grant 24K08626) from the MEXT of Japan and the Adaptable and Seamless Technology Transfer Program through Target-driven R&D (A-STEP) from the Japan Science and Technology Agency (JST). Mutmainaha thanks the International Graduate Program (IGP), Hokkaido University for the scholarship.

Author contributions

YM and KM designed the experimental protocols and drafted the manuscript. Mutmainah and SK performed the synthesized malabaricone C and its derivatives. AS, MS, YO, and HS performed the biological assays for antiviral activity. AK, AF, RK, and Mutmainah performed visualization experiments on sphingomyelin distribution. YM and KM designed the study and wrote the manuscript. All the authors have read and approved the final version of the manuscript.

Competing interests

The authors declare no competing interests.

Additional information

Supplementary Information The online version contains supplementary material available at https://doi.org/10.1038/s41598-024-83633-8.

Correspondence and requests for materials should be addressed to Y.M., A.S. or K.M.

Reprints and permissions information is available at www.nature.com/reprints.

Publisher's note Springer Nature remains neutral with regard to jurisdictional claims in published maps and institutional affiliations.